

Engineered Holliday Junctions as Single-Molecule Reporters for Protein–DNA Interactions with Application to a MerR-Family Regulator

Susanta K. Sarkar,[†] Nesha May Andoy,[†] Jaime J. Benítez,[†] Peng R. Chen,[‡] Jason S. Kong,[†] Chuan He,[‡] and Peng Chen^{*†}

Contribution from the Department of Chemistry and Chemical Biology, Baker Laboratory, Cornell University, Ithaca, New York 14853, and Department of Chemistry, University of Chicago, 929 East 57th Street, Chicago, Illinois 60637

Received April 10, 2007; E-mail: pc252@cornell.edu

Abstract: Protein–DNA interactions are essential for gene maintenance, replication, and expression. Characterizing how proteins interact with and change the structure of DNA is crucial in elucidating the mechanisms of protein function. Here, we present a novel and generalizable method of using engineered DNA Holliday junctions (HJs) that contain specific protein-recognition sequences to report protein–DNA interactions in single-molecule FRET measurements, utilizing the intrinsic structural dynamics of HJs. Because the effects of protein binding are converted to the changes in the structure and dynamics of HJs, protein–DNA interactions that involve small structural changes of DNA can be studied. We apply this method to investigate how the MerR-family regulator PbrR691 interacts with DNA for transcriptional regulation. Both apo- and holo-PbrR691 bind the stacked conformers of the engineered HJ, change their structures, constrain their conformational distributions, alter the kinetics, and shift the equilibrium of their structural dynamics. The information obtained maps the potential energy surfaces of HJ before and after PbrR691 binding and reveals the protein actions that force DNA structural changes for transcriptional regulation. The ability of PbrR691 to bind both HJ conformers and still allow HJ structural dynamics also informs about its conformational flexibility that may have significance for its regulatory function. This method of using engineered HJs offers quantification of the changes both in structure and in dynamics of DNA upon protein binding and thus provides a new tool to elucidate the correlation of structure, dynamics, and function of DNA-binding proteins.

Introduction

Protein–DNA interactions are fundamentally important for gene replication, transcription, recombination, and regulation.¹ Quantifying how proteins interact with and change the structure of DNA is essential in elucidating the mechanisms of their biological functions. Single-molecule techniques,^{2–22} in particular single-molecule fluorescence resonance energy transfer

(smFRET),^{3,6,23} have recently proven to be powerful in defining the correlation of the structure, dynamics, and function of nucleic acid processing proteins. By attaching a FRET donor–acceptor pair to suitable locations on nucleic acids or proteins, smFRET measurements have quantified conformational dynamics of nucleic acids and proteins in real time^{8,18,24–26} and elucidated DNA replication and transcription mechanisms.^{27,28} Experimentally, smFRET techniques rely largely on detecting nanometer-scale structural changes. This is inherently related to both the FRET mechanism and the fluorescent probes suitable for single-molecule detection.^{29,30} However, many DNA-binding proteins

[†] Cornell University.

[‡] University of Chicago.

- (1) Cooper, G. M. *The Cell, A Molecular Approach*, 1st ed.; ASM Press: Washington, 1997.
- (2) Moerner, W. E. *J. Phys. Chem. B* **2002**, *106*, 910–927.
- (3) Michalet, X.; Weiss, S.; Jaeger, M. *Chem. Rev.* **2006**, *106*, 1785–1813.
- (4) Xie, X. S.; Trautman, J. K. *Annu. Rev. Phys. Chem.* **1998**, *49*, 441–480.
- (5) Cornish, P. V.; Ha, T. *ACS Chem. Biol.* **2007**, *2*, 53–61.
- (6) Zhuang, X. *Annu. Rev. Biophys. Biomol. Struct.* **2005**, *34*, 399–414.
- (7) Barbara, P. F., Ed. *Acc. Chem. Res.* **2005**, *38*, Issue 7.
- (8) Liu, H.-W.; Cosa, G.; Landes, C. F.; Zeng, Y.; Kovaleski, B. J.; Mullen, D. G.; Barany, G.; Musier-Forsyth, K.; Barbara, P. F. *Biophys. J.* **2005**, *89*, 3470–3479.
- (9) Forkey, J. N.; Quinlan, M. E.; Goldman, Y. E. *Prog. Biophys. Mol. Biol.* **2000**, *74*, 1–35.
- (10) Nie, S.; Chiu, D. T.; Zare, R. N. *Science* **1994**, *266*, 1018–1021.
- (11) Talaga, D. S.; Lau, W. L.; Roder, H.; Tang, J.; Jia, Y.; DeGrado, W. F.; Hochstrasser, R. M. *Proc. Natl. Acad. Sci. U.S.A.* **2000**, *97*, 13021–13026.
- (12) Levene, M. J.; Korlach, J.; Turner, S. W.; Foquet, M.; Craighead, H. G.; Webb, W. W. *Science* **2003**, *299*, 682–686.
- (13) Lipman, E. A.; Schuler, B.; Bakajin, O.; Eaton, W. A. *Science* **2003**, *301*, 1233–1235.
- (14) Yildiz, A.; Selvin, P. R. *Acc. Chem. Res.* **2005**, *38*, 574–582.

- (15) Amitani, I.; Baskin, R. J.; Kowalczykowski, S. C. *Mol. Cell* **2006**, *23*, 143–148.
- (16) Haran, G. *J. Phys.: Condens. Matter* **2003**, *15*, R1291–R1317.
- (17) Tan, X.; Nalbant, P.; Touthkine, A.; Hu, D.; Vorpapel, E. R.; Hahn, K. M.; Lu, H. P. *J. Phys. Chem. B* **2004**, *108*, 737–744.
- (18) Chen, Y.; Hu, D.; Vorpapel, E. R.; Lu, H. P. *J. Phys. Chem. B* **2003**, *107*, 7947–7956.
- (19) Antikainen, N. M.; Smiley, R. D.; Benkovic, S. J.; Hammes, G. G. *Biochemistry* **2005**, *44*, 16835–16843.
- (20) Zhang, Z.; Rajagopalan, P. T. R.; Selzer, T.; Benkovic, S. J.; Hammes, G. G. *Proc. Natl. Acad. Sci. U.S.A.* **2004**, *101*, 2764–2769.
- (21) Brender, J. R.; Dertouzos, J.; Ballou, D. P.; Massey, V.; Palfey, B. A.; Entsch, B.; Steel, D. G.; Gafni, A. *J. Am. Chem. Soc.* **2005**, *127*, 18171–18178.
- (22) Greene, E. C.; Mizuuchi, K. *J. Biol. Chem.* **2004**, *279*, 16736–16743.
- (23) Myong, S.; Stevens, B. C.; Ha, T. *Structure* **2006**, *14*, 633–643.
- (24) Ha, T. *Biochemistry* **2004**, *43*, 4055–4063.

such as MerR-family regulators involved in transcriptional regulations^{31–35} may not cause DNA structural changes of large enough magnitude for smFRET to detect. A method that enables single-molecule study of protein–DNA interactions while alleviating this hindrance is therefore desirable. Here, we report a novel and generalizable method based on engineered DNA Holliday junctions (HJs) as single-molecule reporters in smFRET measurements for protein–DNA interactions, applied to a MerR-family regulator.^{31–33,36–39}

MerR-family regulators respond to many environmental stimuli, such as heavy metals, antibiotics, or oxidative stress, with high selectivity and sensitivity and regulate gene transcription allosterically.^{31–33,36–39} These regulators operate via a unique DNA distortion mechanism.^{31,33,38,40} They bind tightly to specific dyad symmetric sequences within the spacer region of a promoter both in the absence and in the presence of the effector. Without the effector, the regulator bends DNA, at which the transcription is suppressed. With the effector, the regulator bends and unwinds DNA, which leads to transcription activation. This mechanism was supported by the crystal structures of two MerR-family regulators BmrR and MtaN, both of which are in their activated forms in complex with DNA.^{40,41} The structures of these two regulators show their DNA binding domains undergo small hinging and twisting movements with magnitudes of ~ 6 Å and $\sim 11^\circ$, respectively, forcing DNA bending ($\sim 50^\circ$) and unwinding ($\sim 30^\circ$). We are interested in the dynamic aspects of transcriptional regulation by MerR-family regulators and aim to understand how these regulators interact with DNA and change DNA structures in real time on a single-molecule basis. In this study, we use PbrR691, a Pb^{2+} -responsive MerR-family regulator from *Ralstonia metallidurans*,^{36,39} for proof-of-principle experiments of studying protein–DNA interactions using our new method.

Results and Discussion

Methodology. Figure 1A depicts our method of using engineered HJs as single-molecule reporters in smFRET measurements for PbrR691–DNA interactions. HJs are four-way

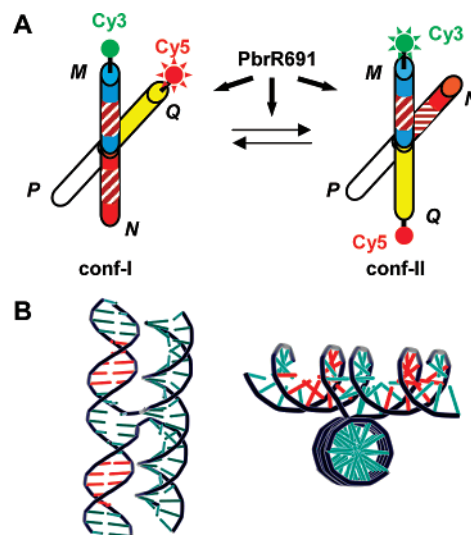


Figure 1. Engineered Holliday junctions (HJs) as single-molecule protein–DNA interaction reporters. (A) Schematic of the dynamic structural equilibrium of an engineered HJ. The line-patterned parts on arms M and N mark the dyad symmetric sequence recognized by PbrR691. PbrR691 binding will perturb the structures of both conf-I and conf-II, and alter their dynamic equilibrium. (B) Structural model of a stacked HJ conformer in two different orientations. The dyad symmetric sequence for PbrR691 recognition is highlighted in red as in conf-I. The model was created using a HJ crystal structure (pdb code 1DCW)⁴² and extending its arms with B-form DNA structures. A model with the dyad symmetric sequence highlighted as in conf-II is shown in Figure S2.

DNA junctions that form during homologous DNA recombination.^{43–45} In the presence of Na^+ and Mg^{2+} , a HJ folds into two stacked X-shaped conformers by coaxial pairwise stacking of its four helical arms (conf-I and conf-II, Figure 1A,B).^{42–44,46} In one conformer, two of the DNA strands run through a pair of stacked helical arms similarly as in a B-form DNA, while the other two strands exchange between stacked helical pairs (Figure 1B).^{42,46} The four strands switch positions in the other conformer. These two stacked conformers coexist in a dynamic equilibrium at room temperature (Figure 1A). By attaching the FRET donor–acceptor pair Cy3–Cy5 to the ends of two HJ arms, the two stacked HJ conformers can be distinguished and their dynamic interconversions can be visualized in real time readily and uniquely using smFRET measurements, as shown by Ha and co-workers.^{23,44}

Building on the structural dynamics of HJs and on the ease of following them by smFRET, our experimental design is to engineer a HJ by encoding in two of its arms the dyad symmetric sequence recognized by PbrR691 (Figure 1). Because the encoded sequence has different spatial orientations (Figure 1A,B), PbrR691 should bind to the two conformers differentially and cause changes in their structures and dynamics. These changes in a single HJ should be readily measurable in real time by smFRET measurements and will thus report how PbrR691 interacts with HJ, that is, DNA, on a single-molecule basis.

This method of using engineered HJs as single-molecule reporters is in principle generalizable because we can encode

- (25) Bokinsky, G.; Rueda, D.; Misra, V. K.; Rhodes, M. M.; Gordus, A.; Babcock, H. P.; Walter, N. G.; Zhuang, X. *Proc. Natl. Acad. Sci. U.S.A.* **2003**, *100*, 9302–9307.
- (26) Rueda, D.; Bokinsky, G.; Rhodes, M. M.; Rust, M. J.; Zhuang, X.; Walter, N. G. *Proc. Natl. Acad. Sci. U.S.A.* **2004**, *101*, 10066–10071.
- (27) Myong, S.; Rasnik, I.; Jool, C.; Lohman, T. M.; Ha, T. *Nature* **2005**, *437*, 1321–1325.
- (28) Margeat, E.; Kapanidis, A. N.; Tinnefeld, P.; Wang, Y.; Mukhopadhyay, J.; Ebright, R. H.; Weiss, S. *Biophys. J.* **2006**, *90*, 1419–1431.
- (29) Ha, T. *Methods* **2001**, *25*, 78–86.
- (30) Weiss, S. *Nat. Struct. Biol.* **2000**, *7*, 724–729.
- (31) Brown, N. L.; Stoyanov, J. V.; Kidd, S. P.; Hobman, J. L. *FEMS Microbiol. Rev.* **2003**, *27*, 145–163.
- (32) O’Halloran, T. V.; Frantz, B.; Shin, M. K.; Ralston, D. M.; Wright, J. G. *Cell* **1989**, *56*, 119–129.
- (33) Frantz, B.; O’Halloran, T. V. *Biochemistry* **1990**, *29*, 4747–4751.
- (34) Busenlehner, L.; Pennella, M. A.; Giedroc, D. P. *FEMS Microbiol. Rev.* **2003**, *27*, 131–143.
- (35) Barkey, T.; Miler, S. M.; Summers, A. O. *FEMS Microbiol. Rev.* **2003**, *27*, 355–384.
- (36) Chen, P.; Greenberg, B.; Taghavi, S.; Romano, C.; van der Lelie, D.; He, C. *Angew. Chem., Int. Ed.* **2005**, *44*, 2715–2719.
- (37) Chen, P.; He, C. *J. Am. Chem. Soc.* **2004**, *126*, 728–729.
- (38) Hidalgo, E.; Ding, H.; Demple, B. *Trends Biochem. Sci.* **1997**, *97*, 207–210.
- (39) Mergeay, M.; Monchy, S.; Vallaey, T.; Auquier, V.; Benotmane, A.; Bertin, P.; Taghavi, S.; Dunn, J.; van der Lelie, D.; Wattiez, R. *FEMS Microbiol. Rev.* **2003**, *27*, 385–410.
- (40) Zheleznova, E. E.; Brennan, R. G. *Nature* **2001**, *409*, 378–382.
- (41) Newberry, K. J.; Brennan, R. G. *J. Biol. Chem.* **2004**, *279*, 20356–20362.
- (42) Eichman, B. F.; Vargason, J. M.; Mooers, B. H. M.; Ho, P. S. *Proc. Natl. Acad. Sci. U.S.A.* **2000**, *97*, 3971–3976.

- (43) Lilley, D. M. J. *Q. Rev. Biophys.* **2000**, *33*, 109–159.
- (44) McKinney, S. A.; Declais, A. C.; Lilley, D. M. J.; Ha, T. *Nat. Struct. Biol.* **2003**, *10*, 93–97.
- (45) Mizuuchi, K. *Annu. Rev. Biochem.* **1992**, *61*, 1011–1051.
- (46) Ortiz-Lombardía, M.; González, A.; Eritja, R.; Aymamí, J.; Azorín, F.; Coll, M. *Nat. Struct. Biol.* **1999**, *6*, 913–917.

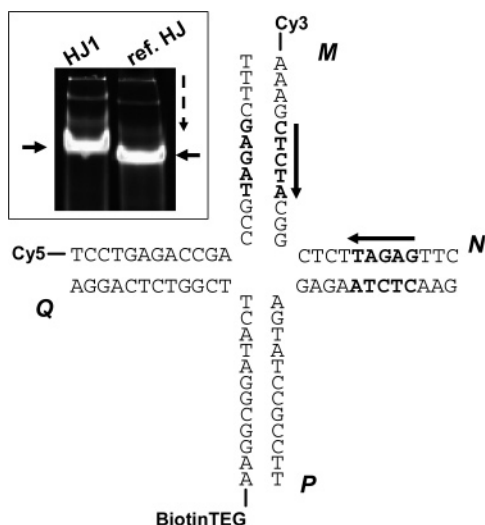


Figure 2. Sequence design and labeling of the engineered HJ1. The dyad symmetric sequence specific for PbrR691 is in boldface and marked by arrows. Inset: PAGE image of HJ1 and a reference HJ (J7) from McKinney et al.⁴⁴ Dashed arrow marks the migration direction. HJ1 is four base pairs larger than the reference HJ and thus migrates slightly slower.

into HJs various sequences recognizable by many DNA-binding proteins. Because protein–DNA interactions are converted to the changes in the structure and dynamics of specifically engineered HJs, it is now possible to use smFRET to study interactions that involve small structural changes.

In the following, we present an engineered HJ specifically designed to bind with PbrR691. We use smFRET measurements to study how PbrR691 distorts HJ structure and changes the kinetics and equilibrium of HJ structural dynamics. The results are used to map the changes imposed by PbrR691 on the potential energy surface of the HJ, and to offer insight into how PbrR691 acts on DNA for transcriptional regulation.

Construction of an Engineered HJ. Figure 2 shows the design of the engineered HJ (referred to as HJ1) using four oligo-DNA strands with Cy3 and Cy5 attached at the 5'-ends of two strands. A biotin-TEG (TEG = tetraethyleneglycol) is also attached to a third strand for immobilization in smFRET measurements. The TEG linker allows freedom for HJ1 structural motions while immobilized. The sequences were designed to contain the PbrR691-specific dyad symmetric sequence spanning arms M and N of HJ1 and to facilitate HJ1 assembly. Gel electrophoresis (Figure 2, inset) and absorption measurements of Cy3–Cy5 spectral features (Figure S3) confirmed the formation of HJ1.

PbrR691–HJ1 Interaction Dynamics. The structural dynamics of a HJ1 molecule is clear from its fluorescence trajectories, which show anticorrelated, two-state fluctuations of Cy3 and Cy5 intensities (Figure 3A). The calculated E_{FRET} trajectory shows reversible transitions between a high E_{FRET} (~ 0.65) and a low E_{FRET} (~ 0.15) state, corresponding to the structural interconversions between conf-I and conf-II, respectively (Figure 1A). Individual waiting times ($t_{\text{conf-I}}$ and $t_{\text{conf-II}}$) in the smFRET trajectories are stochastic, but their distributions are characteristic of and determined by the transition kinetics. The two waiting time distributions from the E_{FRET} trajectories of many HJ1 molecules can be fitted with single-exponential decays (Figure 3B,C), consistent with previous single-molecule studies of HJ structural dynamics.⁴⁴ The rate constants deter-

mined for HJ1 structural interconversions are $k_{\text{I-II}} = 0.20 \pm 0.01 \text{ s}^{-1}$ and $k_{\text{II-I}} = 0.58 \pm 0.02 \text{ s}^{-1}$, giving a conf-I/conf-II equilibrium constant $K_{\text{I/II}}$ of $\sim 2.9 \pm 0.3$.

In the presence of PbrR691 without Pb^{2+} bound (i.e., the apo-PbrR691), the fluorescence and E_{FRET} trajectories of a HJ1 molecule show a stronger bias toward conf-I, the high E_{FRET} state (Figure 3D). We fitted each waiting time distribution with a double exponential function (Figure 3E,F). One of the exponential components was fixed at the value of free HJ1 and accounts for the contribution from free HJ1 molecules in the population, while the other was floated and accounts for the apo-PbrR691 bound HJ1 molecules (see below). The determined rate constants for the apo-PbrR691 bound HJ1 are $k'_{\text{I-II}} = 0.17 \pm 0.01 \text{ s}^{-1}$ and $k'_{\text{II-I}} = 1.30 \pm 0.15 \text{ s}^{-1}$, which differ from those of free HJ1. These different rate constants indicate apo-PbrR691 alters the kinetics of HJ1 structural interconversions and stabilizes the conf-I relative to conf-II with an increased conf-I/conf-II equilibrium constant ($K'_{\text{I/II}} \approx 7.6 \pm 1.0$).

The histograms of E_{FRET} trajectories, which show the two-state distribution of HJ1 structures, clearly show this equilibrium shift of HJ1 structural dynamics upon apo-PbrR691 binding (Figure 4). The relative intensity of the peak corresponding to conf-I increases with increasing concentrations of the protein, indicating apo-PbrR691 preferentially binds to conf-I of HJ1. To determine the binding affinity of apo-PbrR691 to each of the HJ1 conformers, we further measured the peak area ratios in the histograms of the E_{FRET} trajectories with increasing protein concentrations. Fitting the titration curve yields the two dissociation constants for apo-PbrR691 interaction with conf-I ($K_{\text{D-I}} = 0.8 \pm 0.2 \mu\text{M}$) and with conf-II ($K_{\text{D-II}} = 2.2 \pm 0.8 \mu\text{M}$) (Figure 4B, inset). The higher affinity of apo-PbrR691 to conf-I is consistent with its normal function as a double-strand DNA binding protein. As shown in Figure 1B, conf-I has the arms M and N, which encode the dyad symmetric sequence recognized by PbrR691, coaxially stacked to form a B-form DNA-like structure. ($K_{\text{D-I}}$ and $K_{\text{D-II}}$ are lower than that of apo-PbrR691 binding to a double-strand DNA wild-type sequence, $K_{\text{D}} \approx 40 \text{ nM}$. See discussion later.)

Apo-PbrR691 binding also changes the structures of both HJ1 conformers. In the two-dimensional histograms of $E_{\text{conf-I}}$ and $E_{\text{conf-II}}$ (Figure 5A and Figure S4), the peak center shifts to slightly higher values in both $E_{\text{conf-I}}$ and $E_{\text{conf-II}}$ in the presence of the protein. The increased $E_{\text{conf-I}}$ and $E_{\text{conf-II}}$ indicate that arms M and Q move closer in both conformers upon protein binding (reference Figure 1A). These structural changes are also consistent with that apo-PbrR691 binds to both conf-I and conf-II and that the second exponential components in the waiting time distributions are from structural interconversions between apo-PbrR691 bound HJ1 conformers (Figure 3E,F).

To further investigate the structural changes of HJ1 upon PbrR691 binding, we moved the Cy5-label from the end of arm Q to that of arm N (Figure 2 and Figure S5). With this alternative labeling scheme (referred to as HJ1a), conf-I has a low E_{FRET} (~ 0.16) while conf-II has a high E_{FRET} (~ 0.74 , reference Figure 1A), reversed from those of HJ1. Upon interaction with apo-PbrR691, $E_{\text{conf-II}}$ of HJ1a decreases (Figure 5B and Figure S6), showing that the protein widens the angle between arms M and N of conf-II. The behavior of HJ1a in comparison to HJ1 (Figure 5A,B) also confirms that the two-

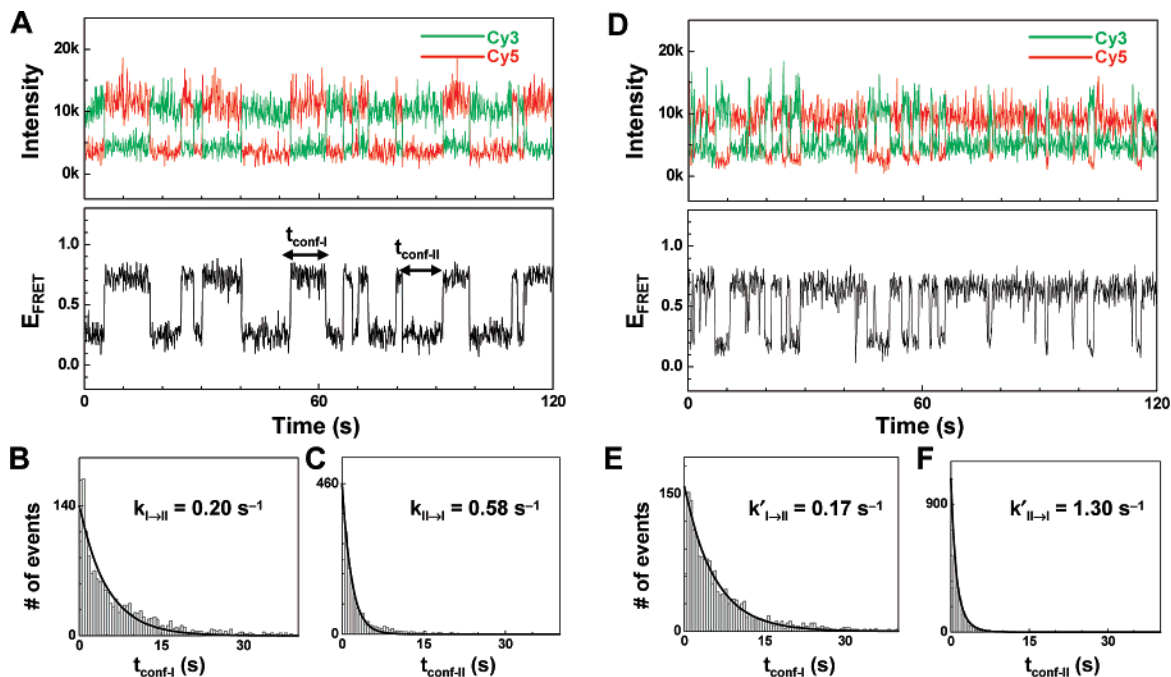


Figure 3. Single-molecule fluorescence and E_{FRET} trajectories, and waiting time distributions. E_{FRET} was calculated as $I_{\text{Cy5}}/(I_{\text{Cy3}} + I_{\text{Cy5}})$, a good approximation for FRET efficiency. (A–C) Free HJ1 (224 molecules analyzed with mean trajectory length of 193 s and standard deviation of 96 s). (D–F) HJ1 in the presence of 2.4 μM apo-PbrR691 (225 molecules analyzed with mean trajectory length of 173 s and standard deviation of 100 s). Bin size: 0.5 s. Solid lines in (B,C) are fits with $y = A \exp(-kt)$. Solid lines in (E,F) are fits with $y = A \exp(-kt) + A' \exp(-k't)$. Fit parameters: (B) $A = 140 \pm 6$, $k = 0.20 \pm 0.01 \text{ s}^{-1}$; (C) $A = 460 \pm 12$, $k = 0.58 \pm 0.02 \text{ s}^{-1}$; (E) $A = 41 \pm 1$, $k = 0.20 \text{ s}^{-1}$ (fixed), $A' = 117 \pm 3$, $k' = 0.17 \pm 0.01 \text{ s}^{-1}$; (F) $A = 478 \pm 24$, $k = 0.58 \text{ s}^{-1}$ (fixed), $A' = 534 \pm 27$, $k' = 1.30 \pm 0.15 \text{ s}^{-1}$.

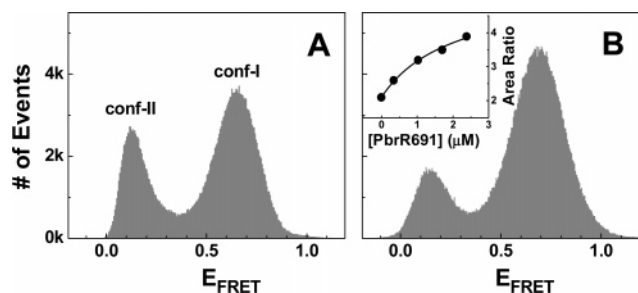


Figure 4. E_{FRET} trajectory histograms of HJ1 in the absence (A) and presence of 2.4 μM apo-PbrR691 (B). Same set of molecules analyzed as in Figure 3. Bin size: 0.005. Note the peak widths in these histograms are unreliable representations of distribution widths as the E_{FRET} trajectories contain significant photon noise. Inset in (B): titration of E_{FRET} peak area ratio (conf-I/conf-II). Solid line: fit with $y = C(1 + [\text{PbrR691}]/K_{\text{D-I}})/(1 + [\text{PbrR691}]/K_{\text{D-II}})$. C is a constant representing the E_{FRET} peak area ratio of free HJ1. See Supporting Information for derivation.

state fluctuations in our single-molecule trajectories are indeed due to Holliday junction structural dynamics.

The widths of the E_{FRET} distributions reflect the conformational distributions of both conformers around their average structures. In Figure 5A (and Figure S4), the distribution of $E_{\text{conf-I}}$ is narrower for HJ1 in complex with apo-PbrR691 than that of free HJ1. The decrease in $E_{\text{conf-II}}$ distribution width is more observable for the alternatively labeled HJ1a (Figure 5B and Figure S6). These decreases in distribution widths indicate apo-PbrR691 constrains the conformational flexibility of both conf-I and conf-II.

We further studied the actions of Pb^{2+} -bound PbrR691 (i.e., the holo-PbrR691) on HJ1. As compared to those of apo-PbrR691, holo-PbrR691 further decreases the rate of the conf-I \rightarrow conf-II transition and increases that of the reverse transition ($k'_{\text{I-II}} = 0.14 \pm 0.01 \text{ s}^{-1}$; $k'_{\text{II-I}} = 1.42 \pm 0.04 \text{ s}^{-1}$, Figure S7),

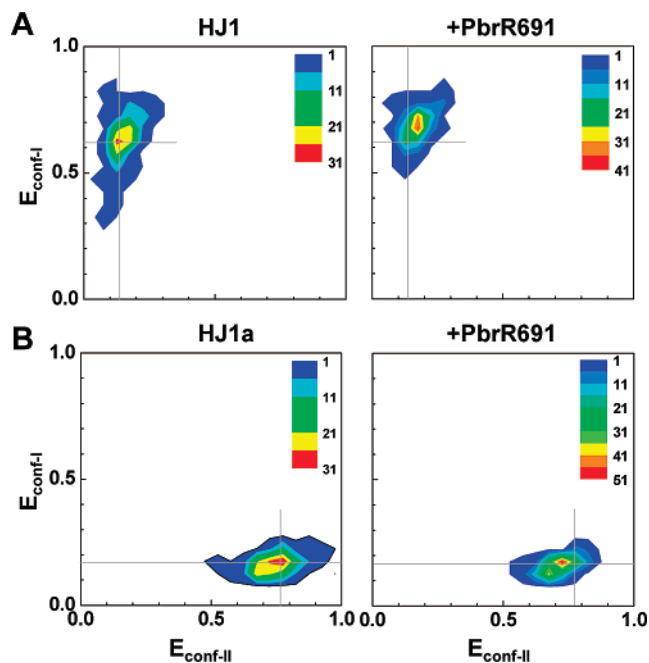


Figure 5. (A) Two-dimensional histograms of $E_{\text{conf-I}}$ and $E_{\text{conf-II}}$ of HJ1 in the absence and presence of 2.4 μM apo-PbrR691. (B) is same as (A) but from the alternatively labeled HJ1a. The E values are the peak centers obtained from fitting individual E_{FRET} histograms of single-molecule trajectories with two Gaussian functions. Each two-dimensional histogram is from data of 220 molecules. Bin size: 0.05.

indicating a slightly larger stabilization of conf-I relative to conf-II ($K'_{\text{I/II}} = 10.1 \pm 0.8$ and Figure S8). The changes in $E_{\text{conf-I}}$ and $E_{\text{conf-II}}$ of HJ1 imposed by holo-PbrR691 are comparable to those caused by apo-PbrR691 (Figure 5A and Figure S9), showing similar structural changes in both conformers. Consistent reduction in the E_{FRET} distribution width of HJ1 was also

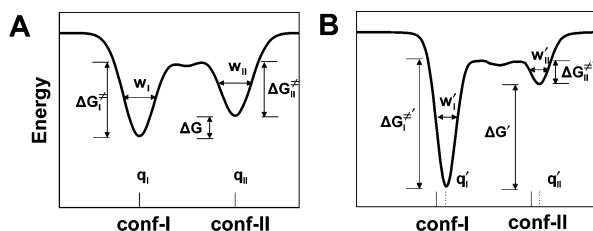


Figure 6. Schematics of potential energy surfaces of (A) HJ1 and (B) HJ1 in complex with apo- or holo-PbrR691. Energetics not drawn to scale.

observed upon interaction with holo-PbrR691 (Figure S9). We also confirmed that Pb^{2+} stays bound to the protein under the condition used in our single-molecule experiments (see Supporting Information).

To show that the interactions between PbrR691 and HJ1 are specific, we performed two control experiments. First, we studied HJ1 in the presence of $5 \mu\text{M}$ CueR, another MerR-family regulator that recognizes a different dyad DNA sequence.^{31,35,47–49} No noticeable perturbations on the HJ1 structural equilibrium and kinetics were observed (Figure S15). Second, we examined the possible interactions of PbrR691 with a Holliday junction (J7 in ref 44) that contains no specific targeting sequences. No noticeable perturbations on J7 structural equilibrium and kinetics were observed in the presence of $2.4 \mu\text{M}$ apo-PbrR691, the highest concentration of PbrR691 in our study (Figure S16). These control experiments confirm that the perturbations of HJ1 structural dynamics by PbrR691 are not due to nonspecific interactions.

Effects of PbrR691 on HJ1 Potential Energy Surfaces (PESs). The above experimental results can map the changes in the PES of HJ1 upon interaction with PbrR691. In the presence of Na^+ and Mg^{2+} , the PES of HJ1 has two dominant potential energy wells corresponding to the two stacked conformers (Figure 6A). Previous studies suggested that a short-lived open structure is an intermediate for HJ structural interconversions, in which the four HJ arms are extended toward the corners of a square.^{43,44} Therefore, a third shallow energy well representing an open structure is included on the PES between the two HJ1 conformers. However, this open structure is undetectable with the solution conditions used to stabilize the stacked HJ1 conformers in our experiments.^{44,50}

Both apo- and holo-PbrR691 cause many changes of the HJ1 PES (Figure 6B). Both forms of PbrR691 decrease the rate constant of the HJ1 $\text{conf-I} \rightarrow \text{conf-II}$ transition and increase that of the reverse transition, with the holo-protein having a larger effect. These altered kinetics indicate PbrR691 changes the free energy barriers for HJ1 conformer interconversion ($\Delta G_{\text{I} \rightarrow \text{II}}^{\text{Pbr}} > \Delta G_{\text{I} \rightarrow \text{II}}^{\text{apo}}$, $\Delta G_{\text{II} \rightarrow \text{I}}^{\text{Pbr}} < \Delta G_{\text{II} \rightarrow \text{I}}^{\text{apo}}$) and, in particular, impairs the transition from conf-I to conf-II. (Note our PES description does not require the structural transitions between PbrR691 bound conformers to occur via the same open structure intermediate of free HJ1.) The changes in energy barriers parallel the thermodynamic equilibrium shifting of HJ1 dynamics toward conf-I, that is, the deepening of the conf-I energy well relative to that of conf-II ($\Delta G' > \Delta G$). Both the kinetics and the

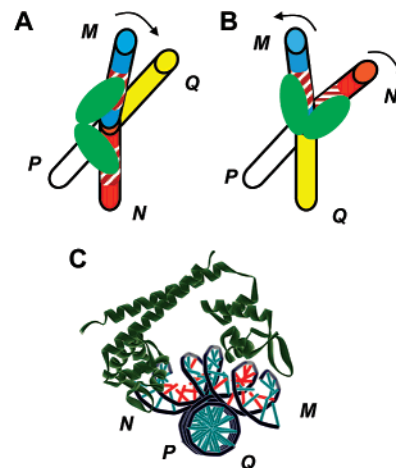


Figure 7. Schemes and models of PbrR691–HJ1 interactions. (A) PbrR691 imposed M–N helix bending of conf-I. (B) PbrR691 caused M–N angle widening of conf-II. (C) Structural model of MtaN (pdb code 1R8D)⁴¹ bound to conf-I of HJ1, showing the bending distortion of the M–N helix.

thermodynamics changes of HJ1 structural dynamics reflect the preference of PbrR691 binding to conf-I, which has the dyad containing M and N arms stacked into a helix.

The structural changes of HJ1 conformers caused by both forms of PbrR691 report the relocation of the energy minima of the two potential energy wells ($q_{\text{I}}' \neq q_{\text{I}}$, $q_{\text{II}}' \neq q_{\text{II}}$). The increased constraints imposed by PbrR691 on the conformational flexibility of both conf-I and conf-II indicate the narrowing of the widths of both potential energy wells ($w_{\text{I}}' < w_{\text{I}}$, $w_{\text{II}}' < w_{\text{II}}$). Both of these effects report the actions of PbrR691 on HJ1 structure that are related to PbrR691 function (discussed below).

The free energy barrier heights, well depths, locations of energy minima, and well widths of PESs are directly correlated to kinetics, thermodynamics, stable structure, and conformational flexibility of HJ1 structural dynamics, respectively. The single-molecule measurements here offer a mapping of PESs before and after protein binding and thus provide an overall picture of the structure–dynamics correlation for PbrR691–HJ1 interactions.

Correlation of PbrR691–HJ1 Interactions to PbrR691 Function. Structural changes imposed by both apo- and holo-PbrR691 bring arms M and Q closer in conf-I of HJ1. In this conformer, the M and N arms, which encode the dyad symmetric sequence recognized by PbrR691, coaxially stack forming a helix that mimics a B-form DNA (Figure 1B).^{42,46} These structural changes can be associated with the M–N helix bending forced by PbrR691, possibly through hinging motions of its DNA-binding domains,^{40,41} leading to a closer distance between the ends of arms M and Q (Figure 7A). This PbrR691-hinging imposed DNA bending is coupled to the transcription regulation by MerR-family regulators, as proposed in the DNA distortion model.^{32,33}

For the alternatively labeled HJ1a, the FRET pair Cy3–Cy5 is attached at the ends of arms M and N and in principle could directly report the bending motions of the M–N helix of conf-I upon PbrR691 binding. However, no significant change in $E_{\text{conf-I}}$ was observed for HJ1a (Figure 5B). Not detecting a significant change in $E_{\text{conf-I}}$ for HJ1a is not surprising, as the end-to-end distance change in bending the M–N helix of conf-I may be small. Assuming a $\sim 130^\circ$ bend angle from the crystal structure of the MtaN–DNA complex,⁴¹ the estimated end-to-

(47) Stoyanov, J. V.; Hobman, J. L.; Brown, N. L. *J. Biol. Chem.* **2001**, *39*, 502–511.

(48) Changela, A.; Chen, K.; Xue, Y.; Holschen, J.; Outten, C. E.; O'Halloran, T. V.; Mondragon, A. *Science* **2003**, *301*, 1383–1387.

(49) Petersen, C.; Moller, L. B. *Gene* **2000**, *261*, 289–298.

(50) Joo, C.; McKinnney, S. A.; Lilley, D. M. J.; Ha, T. *J. Mol. Biol.* **2004**, *341*, 739–751.

end distance change is only ~ 0.8 nm for a 24 base pair DNA helix having a contour length of ~ 8.2 nm. This small distance change is challenging to detect with smFRET measurements. So, instead of trying to detect directly the end-to-end distance changes of the conf-I M–N helix, our approach using engineered HJs circumvents this problem by measuring the distance changes between the ends of arms M and Q. The relative movements of arms M and Q are coupled to M–N helix bending because of the junction connection, thus enabling studies of small bending motions of the DNA helix imposed by PbrR691.

In conf-II, arms M and N form a small angle ($\sim 40^\circ$),^{42,46} and the spatial orientation of the two halves of the dyad symmetric sequence deviates far from that in a double-strand DNA helix (Figure 1A and Figure S2). Therefore, binding to conf-II by both forms of PbrR691 is less favorable, and an angle widening between arms M and N is observed (Figure 7B). This widening of the M–N angle in conf-II and the bending of the stacked M–N helix in conf-I both reflect the actions of PbrR691 on DNA that are coupled to the transcriptional regulation.

Because no structural information is available on PbrR691, the structural data of the MtaN–DNA complex⁴¹ were used to provide a physical picture of the interaction geometry of the PbrR691–HJ1. Figure 7C shows a structural model of MtaN bound to conf-I of HJ1. This model was generated by adjusting and aligning the stacked M–N helix structure with the DNA structure in the MtaN–DNA complex. The structural model indicates that the protein binds to the major grooves at the dyad symmetric sequence and the M–N helix bending leads to a closer distance between the ends of arms M and Q (reference Figure 1B, right), which is consistent with our smFRET measurements of HJ1 interactions with both apo- and holo-PbrR691.

Although PbrR691 binding constrains the conformational flexibility of both HJ1 conformers relative to that of free HJ1 (Figure 5), PbrR691 still allows the structural interconversion of HJ1 between conf-I and conf-II. Considering that PbrR691 binds to both conf-I and conf-II, in which the dyad symmetric sequence has distinct spatial orientations, PbrR691 could stay bound to HJ1 during the structural transitions without dissociation. This would be consistent with that the rate constants, $k'_{I \rightarrow II}$ and $k'_{II \rightarrow I}$, determined from the waiting time distributions in the presence of apo-PbrR691 are independent of the protein concentration within our experimental error (Figure 3E,F and Figure S10). Another possibility is that one of the two DNA-binding domains of PbrR691 could detach from HJ1 during the structural interconversion. The rate constants for this interconversion pathway of HJ1 would also be independent of protein concentration. Complete dissociation of PbrR691 before HJ1 undergoes structural interconversion could also take place, but this possibility cannot be evaluated reliably with our current data (see Supporting Information for discussions and Figure S1). The ability of PbrR691 to bind both conformers, which have drastically different dyad sequence orientations, and to allow HJ1 structural dynamics, which involves large amplitude movements of its helical arms, suggests the conformation of PbrR691, especially of its DNA-binding domains, is flexible. We speculate the conformational flexibility of PbrR691 may play a role in its transcriptional regulation function, such as adopting different conformations to better interact with RNA

polymerase for gene transcription. Further studies are in progress to address this possibility.

The low binding affinities of PbrR691 to the two conformations of HJ1 ($K_{D-I} \approx 0.8 \mu\text{M}$ and $K_{D-II} \approx 2.2 \mu\text{M}$) indicate the method of using engineered HJs is applicable for studying weak protein–DNA interactions. However, as compared to that of PbrR691 binding to a double-strand DNA with wild-type sequence ($K_D \approx 40$ nM, unpublished results), the binding affinity to conf-I is lower and likely because many nucleotides were changed in the sequence between the two halves of the dyad symmetric sequence in designing HJ1 (Figure 2). (The wild-type sequence is 5'-*CTCTATAGTA*ACTAGAG-3', where the dyad sequence is italicized.³¹) The relative orientation of the two halves of the dyad sequence in a DNA helix is also important for binding MerR-family regulators,^{33,40,51} but our model does not show a noticeable difference in their relative orientation in the M–N helix of conf-I from that in a double strand B-form DNA (Figure 1B). The junction structure that resides at the center of the dyad sequence in our design could also adversely affect the PbrR691 affinity. However, previous studies on MtaN indicated the central base pair is not important for its DNA-binding affinity.⁴¹ Therefore, the small structural difference of the junction from a double-strand DNA is less likely a reason for the lower PbrR691 binding affinity. We have designed a second generation of the engineered HJ specific for PbrR691, in which a wild-type sequence is used to span the HJ M–N arms. Studies on this engineered HJ will be reported in the future. Furthermore, no other significant differences were observed between HJ1 interactions with apo-PbrR691 and with holo-PbrR691, except for the larger equilibrium shift to conf-I caused by the holo-protein. This is consistent with that both forms of PbrR691 bend DNA and the expected additional effect of holo-PbrR691 is unwinding of DNA ($\sim 30^\circ$). This unwinding is more challenging to detect than the bending motion with smFRET. We are currently designing a different HJ motif to specifically address small unwinding motions.

Application to Other Regulators. To test the general applicability of our method, we designed another engineered HJ that contains the specific dyad sequence recognized by CueR, a Cu^{1+} -responsive MerR-family regulator that operates similarly to PbrR691 in regulating gene transcription. In the presence of $1.0 \mu\text{M}$ apo-CueR, the structural equilibrium of this engineered HJ significantly shifts toward conf-I, consistent with the observations for HJ1–PbrR691 interactions (Figure S17). This example supports the general applicability of our approach using engineered HJs to probe protein–DNA interactions. The details on the CueR study will be published separately.

Summary

We have developed a novel method using engineered DNA HJs as single-molecule reporters in smFRET measurements to study protein–DNA interactions. Using the MerR-family regulator PbrR691 as a model, we have shown that the engineered HJ1 encoding a PbrR691-targeting sequence reports how both apo- and holo-PbrR691 bind the two stacked HJ1 conformers, change their structures, constrain their conformational distributions, alter their structural transition kinetics, and shift their dynamic structural equilibrium. The information obtained maps

(51) Outten, C. E.; Outten, F. W.; O'Halloran, T. V. *J. Biol. Chem.* **1999**, *274*, 37517–37524.

the potential energy surfaces of HJ1 before and after PbrR691 binding. Because the helical arms of the stacked conformers are structurally similar to B-form DNA, the PbrR691-imposed structural changes of HJ1, in particular of conf-I, reveal the actions of PbrR691 on DNA for transcriptional regulation and reflect the underlying protein motions that force DNA structural changes. The ability of PbrR691 to bind both HJ1 conformers and allow HJ1 structural dynamics also reveals the conformational flexibility of PbrR691 that may have significance for its function in gene transcriptional regulation.

Using engineered HJs as single-molecule reporters is in principle generalizable and applicable to study many other DNA-binding proteins by encoding various sequences into HJ arms. As the effects of protein actions are converted to the changes in the structure and dynamics of HJs, interactions that are weak and only involve small structural changes can be studied by this method. Being able to quantify the changes in structure and dynamics of DNA simultaneously upon protein binding provides a new opportunity to unravel the functional consequences of protein–DNA interactions and elucidate the correlation of structure, dynamics, and function of DNA-binding proteins.

Materials and Methods

HJ Construction and Purification. In HJ1, only two of the four DNA strands have sequences independent of each other. We specified the dyad symmetric sequence in the strand spanning arms M and N, and generated the rest of the sequence of this strand and the sequence of the strand spanning arms P,Q to maximize their orthogonality using the program DNA sequence generator.⁵² Labeled oligomeric DNA strands for HJ1 construction were purchased from Integrated DNA Technologies. HJ1 was assembled by annealing three of the four strands at 60 °C at 10 μ M in a 10 mM pH 7.3 Tris buffer containing 100 mM NaNO₃. The pH of all buffers was adjusted with HNO₃. The solution was then slowly cooled to 37 °C at which the fourth strand was added, incubated for 30 min, and then cooled to room temperature. The assembled HJ1 was further purified by electrophoresis in 20% polyacrylamide gels.

Protein Expression and Purification. PbrR691 was expressed and purified as reported.³⁶ Briefly, PbrR691, cloned in the expression vector pET30b, was expressed in *E. coli* strain BL21 star (DE3). After IPTG induction, cells were harvested and disintegrated by French press. The protein in the supernatant was then purified first via a Heparin affinity column (16/10 Heparin FF, GE healthcare) and then a gel filtration column (HILOAD 26/60 Superdex 200 PR, GE healthcare) using a GE AKTA FPLC. The protein purity was checked by SDS-PAGE, identity confirmed by ESI-MS, and concentration quantitated by BCA protein assay (Pierce). All protein samples were stored at –80 °C in 10 mM Tris buffer, pH 7.3, containing 500 mM NaNO₃, 20% glycerol, and 5 mM β -mercaptoethanol.

Single-Molecule Measurements and Data Analyses. Single-molecule fluorescence measurements were performed on a home-built prism-type total internal reflection microscope based on an Olympus IX71 inverted microscope. A continuous wave circularly polarized 532 nm laser beam (CrystalLaser, GCL-025-L-0.5%) of 1–5 mW was focused onto an area of $\sim 150 \times 75 \mu\text{m}^2$ on the sample to directly excite the Cy3 probe. The fluorescence of both Cy3 and Cy5 was collected by a 60X NA1.2 water-immersion objective (UPLSAPO60XW, Olympus), filtered to reject laser light (HQ550LP), and split by a dichroic mirror (635DCXR) into two channels using a Dual-View system (Optical Insights, Inc.). Each channel of fluorescence was further filtered (HQ580-60m or HQ660LP) and projected onto half of the imaging area of a camera (Andor iXon EMCCD, DV887DCS-BV), controlled by an Andor IQ software. All optical filters are from Chroma Technology Corp.

A flow cell, formed by double-sided tapes sandwiched between a quartz slide (Technical Glass or Finkenbeiner) and a borosilicate coverslip (Gold Seal), was used to hold aqueous sample solutions for single-molecule fluorescence measurements. All samples were in 10 mM Tris buffer, pH 7.3, 100 mM NaNO₃, 50 mM Mg(NO₃)₂ unless indicated otherwise. To minimize nonspecific protein adsorption on glass surfaces, quartz slides were first amine functionalized (Vectabond, Vector Laboratories) and then coated with PEG polymers (100 mg/mL m-PEG-SPA-5000 and 1 mg/mL biotin-PEG-NHS-3400, Nektar Therapeutics).^{53,54} 1% of the PEG polymers contain a biotin terminal group to form biotin-streptavidin (Molecular Probes) linkages for immobilizing biotinylated HJ1 molecules (Figure S11). Oxygen scavenging system (0.1 mg/mL glucose oxidase (Sigma), 0.025 mg/mL catalase (Roche), 4% glucose (Aldrich), and 1 mM Trolox (Sigma))⁵⁵ was added into the sample solution just before each experiment to prolong the lifetime of the fluorescence probes, and was refreshed during experiments every half an hour.

Acknowledgment. We thank Dr. Z. Huang and Q. Wang for preliminary studies, Dr. H. Babcock and Prof. X. Zhuang for sharing a microscope design and an IDL program, and Prof. T. Ha for a preprint.⁵⁵ This research was supported in part by Cornell University (P.C.), a Camille and Henry Dreyfus New Faculty Award (P.C.), an NIH Molecular Biophysics Training Grant (J.J.B.), and the National Science Foundation (C.H.).

Supporting Information Available: Control experiment on Pb²⁺ binding to PbrR691, waiting time distribution analyses, statistical analyses of single-molecule E_{FRET} values, control experiments for PbrR691–HJ1 interaction specificity, and an application of engineered HJ to study CueR–DNA interactions. This material is available free of charge via the Internet at <http://pubs.acs.org>.

JA072485Y

(52) Feldkamp, U.; Saghafi, S.; Banzhaf, W.; Rauhe, H. In *DNA7: LNCS*; Jonoska, N., Seeman, N. C., Eds.; Springer-Verlag: Berlin, 2002; Vol. 2340, pp 23–32.

(53) Rasnik, I.; McKinney, S. A.; Ha, T. *Acc. Chem. Res.* **2005**, *38*, 542–548.

(54) Rasnik, I.; Myong, S.; Cheng, W.; Lohman, T. M.; Ha, T. *J. Mol. Biol.* **2004**, *336*, 395–408.

(55) Rasnik, I.; McKinney, S. A.; Ha, T. *Nat. Methods* **2006**, *3*, 891–893.